JACS
JOURNAL OF THE AMERICAN CHEMICAL SOCIETY

ARTICLE

pubs.acs.org/JACS

Endocyclic Cleavage in Glycosides with 2,3-*trans* Cyclic Protecting Groups

Hiroko Satoh,[*,†] Shino Manabe,[*,‡] Yukishige Ito,[‡] Hans P. Lüthi,[§] Teodoro Laino,[∥] and Jürg Hutter[⊥]

[†]National Institute of Informatics (NII), Tokyo 101-8430, Japan

[‡]RIKEN Advanced Science Institute, Saitama 351-0198, Japan

[§]Laboratory of Physical Chemistry, Swiss Federal Institute of Technology (ETH), 8093 Zürich, Switzerland

[∥]IBM Research - Zurich, 8803 Rüschlikon, Switzerland

[⊥]Institute of Physical Chemistry, University of Zurich, 8057 Zürich, Switzerland

Supporting Information

ABSTRACT: An endocyclic pathway is proposed as a reaction mechanism for the anomerization from the β (1,2-*trans*) to the α (1,2-*cis*) configuration observed in glycosides carrying 2,3-*trans* cyclic protecting groups. This reaction occurs in the presence of a weak Lewis or Brønsted acid, while endocyclic cleavage (endocleavage) in typical glycosides was observed only when mediated by protic media or strong Lewis acids. To rationalize the behavior of this class of compounds, the reaction mechanism and the promoting factors of the endocleavage are investigated using quantum-mechanical (QM) calculations and experimental studies. We examine anomerization reactions of thioglycosides carrying 2,3-*trans* cyclic protecting groups, employing boron trifluoride etherate ($BF_3 \cdot OEt_2$) as a Lewis acid. The estimated theoretical reactivity, based on a simple model to predict transition state (TS) energies from the strain caused by the fused rings, is very close to the TS energies calculated by the TS search along the C1−C2 bond rotation after the *endo* C−O bond breaking. Excellent agreement is found between the predicted TS energies and the experimental reactivity ranking. The series of calculations and experiments strongly supports the predominance of the endocyclic rather than the exocyclic mechanism. Furthermore, these investigations suggest that the inner strain is the primary factor enhancing the endocleavage reaction. The effect of the cyclic protecting group in restricting the pyranoside ring to a $^4C_1$ conformation, extensively discussed in conjunction with the stereoelectronic effect theory, is shown to be a secondary factor.

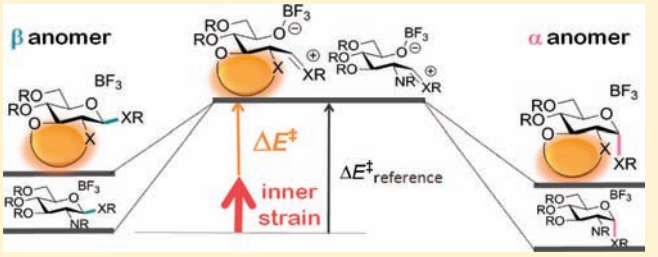

1. INTRODUCTION

Carbohydrates, ubiquitously present in living-organisms, play an important role in biological systems. To unravel the mechanistic details of their reactivity, experimental and theoretical studies have been performed extensively in the context of glycoscience and chemical biology.[1,2] Although the chemistry of carbohydrates has been well understood, there is a long-standing open issue regarding the hydrolytic cleavage sites in pyranosides, known as the "exocyclic vs endocyclic question" (Figure 1). Because of their unsymmetrical nature, pyranosides can undergo hydrolytic cleavage through either an exocyclic or endocyclic pathway. In the first case, the exocyclic bond, between the anomeric carbon C1 and the exocyclic oxygen O1 (or sulfur S1 for thioglycosides), breaks. This pathway, known also as exocyclic cleavage or exocleavage, leads to a cyclic oxacarbenium ion, which is the intermediate of glycosylation reactions.[3−9] In the second one, the endocyclic bond between the anomeric carbon C1 and the endocyclic oxygen O5 in the pyranose ring breaks. This pathway leads to an acyclic oxacarbenium ion and is known as endocyclic cleavage or endocleavage.[10−32] While the

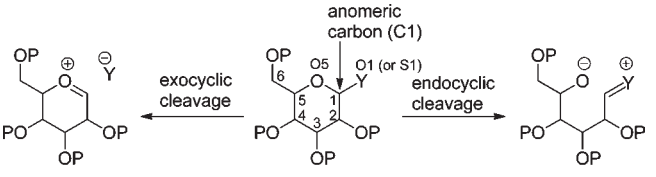

Figure 1. Exocyclic vs endocyclic question.

endocleavage is unanimously considered to be a minor cleavage mode for pyranosides, the exocleavage plays the role of major reactivity channel in organic synthesis. Nonetheless, a way to promote the endocyclic pathway is highly desirable because it will

Received: February 1, 2011
Published: March 21, 2011

dx.doi.org/10.1021/ja201024a | J. Am. Chem. Soc. 2011, 133, 5610–5619

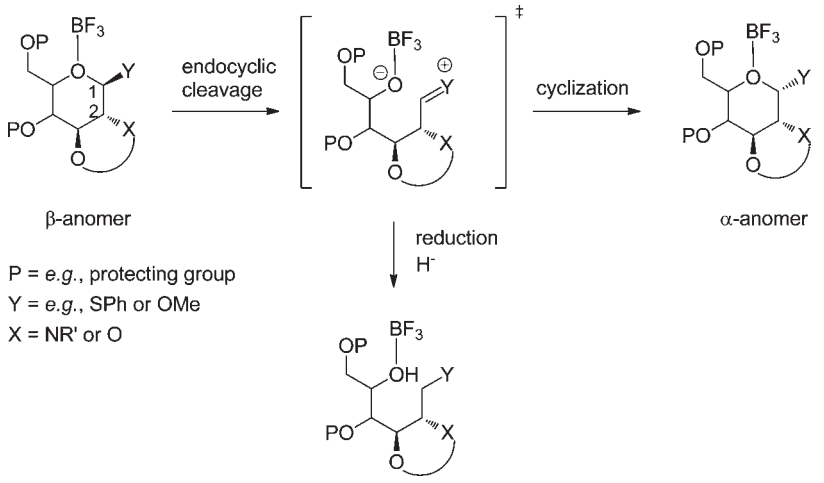

Figure 2. Proposed pathway of the anomerization reactions of pyranosides with 2,3-*trans* cyclic protecting groups. Experiments and computations suggest the endocyclic pathway. The reaction is initiated by BF_3 approaching the ring oxygen, activating the endocyclic C−O bond cleavage (endocleavage). As the bond breaking proceeds, the C1−C2 bond consecutively rotates, reaching the α-anomer by recyclization via the transition state.[30] Acyclic intermediates produced by endocleavage were captured in experiments.[29].

allow the invention of new strategies for the highly stereoselective synthesis of several oligosaccharides.

The first investigation on endocleavage of pyranosides dates back to the work on the hydrolysis of 3:6-anhydro-methyl glucosides reported by Haworth in 1941.[10] Several decades later, the first reports on the theoretical investigations of the C−O bond cleavage were published by Gorenstein et al.[11] They discussed the stereoeletronic control in carbon−oxygen and phosphorus−oxygen bond breaking processes with ab initio quantum-mechanical calculations. Subsequently, within an exocyclic vs endocyclic debate on the hydrolysis of oligosaccharides in a lysozyme complex,[11,13,33−39] Post, Karplus, Phillipes, and co-workers suggested an endocyclic mechanism using classical molecular dynamics simulations. Their findings were supported by the conformational analysis of the crystal structure of a puckered pyranoside adopting a $^4C_1$ conformation in the active site of lysozyme.[13,14] Afterward, Ram and Franck captured a cation produced via endocleavage during alkyl β-THP acetal methanolysis by an intramolecular aza-Diels−Alder reaction,[15] while Fraser-Reid et al. submitted the experimental evidence of an endocleavage process, taking place during the acetolysis of the acyl-protected methyl glycosides in presence of ferric chloride.[17] Only in 1994, Anslyn and co-workers examined the exocyclic vs endocyclic problem using β-alkyl acetal probes of a *cis*-decalin type, via deuterium scrambling for solvolysis (in methanol or aqueous media).[18,20] They concluded that the endocyclic pathway exists as well as the exocyclic pathway at least for the acetal probes. Several works have been published in subsequent years, both theoretical and experimental, supporting the existence of an endocyclic pathway under protic media or strong Lewis acid conditions. Deslongchamps and Dory investigated reaction pathways of enzyme-catalyzed hydrolysis of glycosides based on quantum-mechanical calculations as well as experimental study.[22] There are systematic analyses on endocleavage of glycosides by Frejd et al.[21] and by Murphy and co-workers.[26,32]

Only recently, an endocyclic pathway was proposed by Crich,[23] Oscarson,[24,27] and Manabe,[25,29−31] independently, as a reaction mechanism for anomerization reactions from the β (1,2-*trans*) to the α (1,2-*cis*) anomer,[40] observed in pyranosides carrying 2*N*,3*O*-*trans*-oxazolidinone groups in the presence of $BF_3 \cdot OEt_2$. If this anomerization reaction really occurs via an endocyclic pathway, this is the first case of endocleavage of pyranosides under weak acidic conditions. In fact, it was generally assumed that protic media or strong Lewis acids (e.g., $SnCl_4$ or Me_2BBr) were necessary to activate pyranosides to undergo endocleavage.

The general hypothesis for the anomerization starts with the endocleavage followed by bond rotation and final cyclization (Figure 2). Experimental and theoretical investigations strengthen the relevancy of the predominance of endocleavage. Oscarson and co-workers inferred an endocyclic mechanism from experimental outcomes on anomerization reactions from the β- to the α-linkage for 2-*N*-acetyl-2*N*,3*O*-oxazolidinone-protected glucosamines.[27] Experimental evidence of the existence of the endocleavage pathway in pyranosides carrying 2,3-*trans* carbamate or carbonate was demonstrated observing the adducts of the acyclic cations produced via endocleavage, captured by reduction, chloridation, and inter- or intramolecular Friedel−Crafts reactions.[29] In theoretical studies, density functional theory (DFT) calculations demonstrated that pyranosides, carrying the cyclic protecting groups, undergo endocleavage-induced anomerization more easily than typical pyranosides.[30] A solvent effect was also observed to play a role in the anomerization reactions.[31] In fact, in comparison with the reaction in dichloromethane, the reaction is accelerated and decelerated in acetonitrile and diethyl ether solvents, respectively. Interestingly, it was reported that anomerization does not occur in pyranosides with 2,3-*cis* carbonate.[29]

An open issue is the identification of the predominant factor enhancing endocleavage in the class of pyranosides with cyclic protecting groups. The stereoelectronic effect theory is often used to discuss the feasibility of exocyclic vs endocyclic cleavage.[11−18,20,22,41] The preferential conformations of a pyranose ring can influence the stereoelectronic contribution. According to the stereoelectronic effect theory, an exocyclic C−X (*X* = e.g., O, S) bond in a (pseudo)axial orientation enhances exocleavage, whereas a C−X bond in a (pseudo) equatorial orientation makes exocleavage energetically unfavorable. In the case of pyranosides carrying 2,3-*trans* cyclic protecting groups, the pyranoside ring will be locked into a

dx.doi.org/10.1021/ja201024a | *J. Am. Chem. Soc.* 2011, 133, 5610–5619

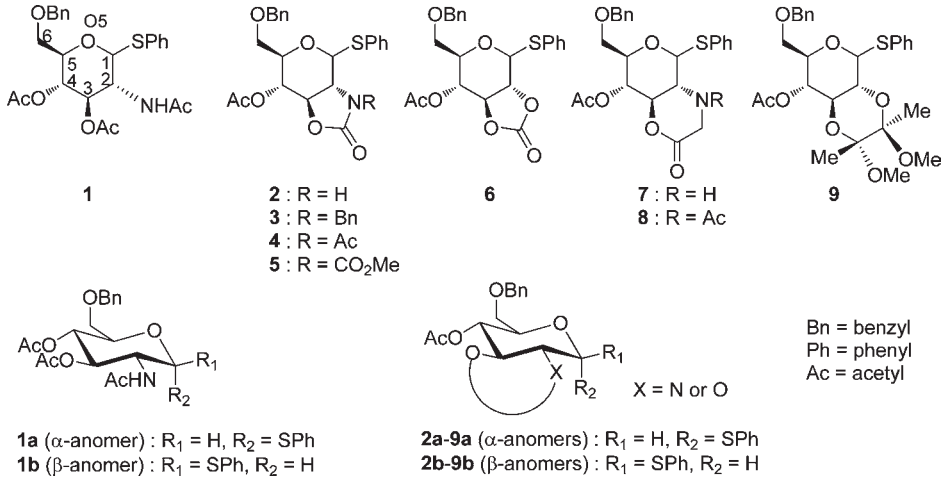

Figure 3. Set of compounds designed for the investigation. The α- and the β-anomers are represented as **a** and **b** with the structure no., respectively (e.g., **1a** and **1b**).

$^4C_1$ conformation by the fused protecting ring. For the β-anomer in this conformation, the exocyclic C−X bond is in an equatorial orientation. Therefore, the stereoelectronic contribution has a negative effect on exocleavage and a positive effect on endocleavage. Thus the 2,3-*trans* fused ring stabilizing a $^4C_1$ conformation of the pyranoside ring will promote endocleavage. However, the series of compounds studied here undergo anomerization even under very mild reaction conditions, in some cases showing a perfect anomerization in the presence of a weak Lewis acid at −30 °C. In contrast, the maximum yield of the α-product reported for other known pyranoside compounds is even at room temperature only 30%.[15,18,20] The high reactivity of the series of pyranosides with cyclic protecting groups indicates the existence of other contributing factors.

Based upon detailed investigations on the geometries and experimental observations, we present a model in which the inner strain energy, caused by the two fused rings, is assumed to be the predominant factor responsible for the promotion of endocleavage. This model allows us to formulate a simple expression to predict TS energies from the inner strain of the cyclic protecting group and from the TS anomerization energy of a reference pyranoside without a 2,3-*trans* cyclic protecting group. The predicted values from the inner strain show a good agreement with the TS energies optimized by quantum mechanical methods. The trend of the predicted TS energies agrees with the observed experimental reactivity ranking. These results indicate that the reactivity can be determined from the inner strain considered as the predominant factor. In the present article, we describe the theoretical and experimental studies that identify the predominant factor and lead to the definition of the reactivity predictor.

The model set of compounds designed for the present investigations consists of a common moiety of 4-*O*-acetyl-6-*O*-benzyl-thiophenylglycosides (Figure 3). A typical pyranoside, 3,4-diacetyl-*N*-acetylglucosamine (**1**) was selected as the reference. This does not carry any cyclic protecting group and does not undergo anomerization reaction, either. Out of the pyranosides with cyclic protecting groups that have been thoroughly experimentally studied, we chose the 2*N*,3*O*-*trans*-*N*-substituted oxazolidinone protected glucosamines (**2**−**5**) and a glycoside with 2,3-*trans*-carbonate (**6**). Pyranosides carrying six-membered protecting groups (**7**−**9**) were added to identify the influence of the ring size and the effect of the carbonyl group in the cyclic protecting groups. The pyranoside rings of **2**−**9** are restrained to a $^4C_1$ conformation by the 2,3-*trans* fused ring (**2**−**8**) or by the *trans*-decalin structure (**9**).

2. COMPUTATIONAL METHODS

All calculations were performed using density functional theory (DFT) at the B3LYP/6-31G(d,p) level[42,43] with the Gaussian 03 program.[44] The model structures **1**−**9** were generated via full geometry optimization in the gas phase for the anomeric isomers (anomers) α (**1a**−**9a**) and β (**1b**−**9b**). Optimizations were initiated from an ideal $^4C_1$ conformation (Figure 3). The X-ray structures measured for **3b** and **4b** are in excellent agreement with the calculated geometries.[28,29] This fact demonstrates the high quality of the geometries from the DFT calculations.

We searched transition states (TS) in the gas phase for the glycosides **1**−**4**, **6**, and **9**, restricting the search along the C1−C2 torsion angle θ (H1−C1−C2−H2) as a reaction coordinate.[30] The final TS structures were located using the STQN (Synchronous Transit-Guided Quasi-Newton) method[45,46] by using the QST3 option with three molecule specifications of the β-anomer (reactant), the α-anomer (product), and an optimized TS candidate. The results from the TS theory were validated by comparing them to experimental product yields of the α- and β-anomers. The order of the potential energies of the β-anomer (reactant), the TS structure, and the α-anomer (product) are preserved in a dichloromethane (CH_2Cl_2) solvent as estimated with an IEF-PCM (Integral-Equation Formation-Polarizable Continuum Model)[47] calculation by using the default parameter of Gaussian 03 for this solvent (dielectric permittivity ε = 8.93; see the Supporting Information for details of the results).

Pilot calculations of the energy profile associated with the endocleavage reaction were performed for **1b** and **3b** in the gas phase. We performed constraint geometry optimization, starting from the optimized structures and progressively elongating, in steps of 0.01 nm, the C1−O5 bond from 0.15 nm to 0.27 and to 0.28 nm for **1b** and **3b**, respectively. The final bond lengths are close to the bond lengths at TS (0.269 and 0.278 nm). The amount of energy required to elongate the C1−O5 bond (131.2 and 91.9 kJ·mol^{-1} for **1b** and **3b**, respectively) is very close to the activation energy from the β-anomer to the TS (159.5 and 83.6 kJ·mol^{-1} for **1** and **3**, respectively). The resulting energy

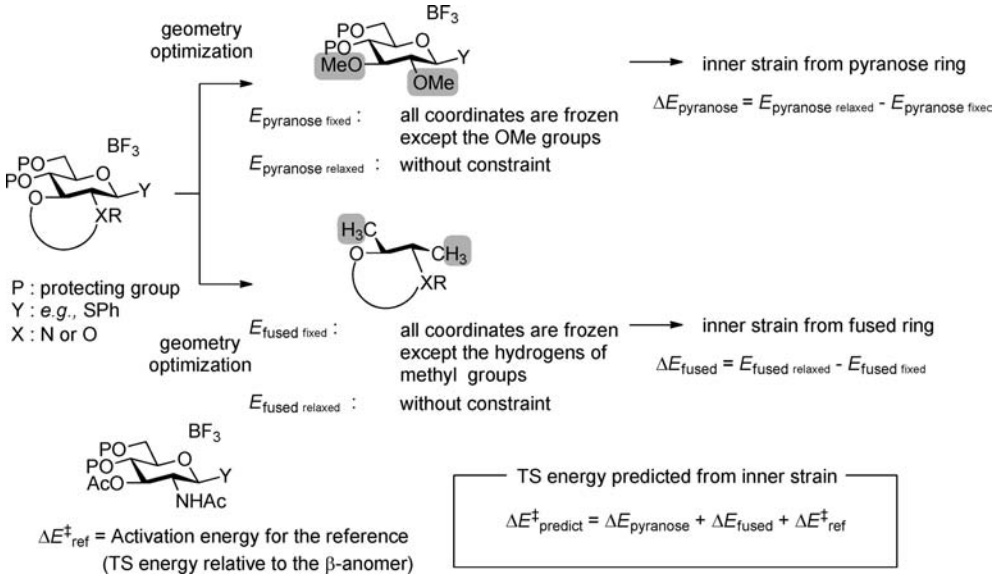

Figure 4. Model to predict TS energies from inner strain.

profile calculation along the C1−C2 bond rotation after the elongation of the C1−O5 bond and using a constraint on the C1−O5 distance (0.27 and 0.28 nm for **1** and **3**), reached states close to the TS via a rather flat potential energy region (from −156.2 to −35.6 degrees, and from −158.8 to −28.8 degrees, respectively). The results indicate that C1−C2 bond rotation is almost free after endocleavage. The important factors enhancing the reactivity should therefore predominantly influence the initiation of the bond breaking rather than the C1−C2 bond rotation.

On the other hand, the pyranoside rings with a 2,3-*trans* cyclic protecting group attached (**2**−**6**, and **8**), which undergo anomerization reaction, were found to be slightly deformed compared with the reference pyranoside **1**. These observations lead us to the assumption that the strain caused by the fused ring is a primal trigger in activating endocleavage. We formulated a simple model to predict TS energies from inner strain (Figure 4). The model assumes that the series of pyranosides have almost the same TS structures and that the TS relative to the β-anomer (reactant) appear to be lower in energy because the inner strain destabilizes the reactants. This model is stimulated by the so-called *extended activation strain model* developed by Bickelhaupt et al.[48−53] In this elegant approach to understanding palladium-induced bond activation, the activation energy is decomposed into the activation strain of the reactants and the stabilizing TS interaction between the reactants. Although their concept for intermolecular reaction systems cannot be applied to our intramolecular anomerization reaction directly, we followed the spirit of the model.

With our new method for the pyranoside system, the activation energy ($\Delta E^{\ddagger}_{\text{predict}}$; the potential energy of TS relative to the β-anomer) is decomposed into the inner strain energy (ΔE_{strain}) and the activation energy of a reference pyranoside ($\Delta E^{\ddagger}_{\text{ref}}$; the potential energy of TS relative to the β-anomer).

$$\Delta E^{\ddagger}_{\text{predict}} = \Delta E_{\text{strain}} + \Delta E^{\ddagger}_{\text{ref}}$$

The inner strain energy is decomposed into a contribution from the pyranose ring ($\Delta E_{\text{pyranose}}$) and one from the fused ring (ΔE_{fused}). Both contributions are calculated as relaxation energies of one ring if the other ring is removed.

$$\Delta E_{\text{strain}} = \Delta E_{\text{pyranose}} + \Delta E_{\text{fused}}$$

In the calculation of $\Delta E_{\text{pyranose}}$, the protecting groups at C2 and C3 are changed to methoxy groups. The difference between the potential energy ($E_{\text{pyranose}_{\text{fixed}}}$), computed by a constrained geometry optimization (where we constrained all atomic coordinates except the methoxy groups), and the potential energy ($E_{\text{pyranose}_{\text{relaxed}}}$), obtained by a full relaxation, is assigned to the inner strain (upper scheme of Figure 4):

$$\Delta E_{\text{pyranose}} = E_{\text{pyranose}_{\text{fixed}}} + E_{\text{pyranose}_{\text{relaxed}}}$$

In the calculation of ΔE_{fused}, C1 and C4 are changed to methyl groups after eliminating the partial structure including C5, C6, and *endo*-oxygen (O5). Similarly to the term described above, the difference between the potential energy ($E_{\text{fused}_{\text{fixed}}}$), computed by a constrained geometry optimization (where we constrained all atomic coordinates except the hydrogen atoms of the methyl groups), and the potential energy ($E_{\text{fused}_{\text{relaxed}}}$), obtained by a full relaxation, is assigned to the inner strain (lower scheme of Figure 4):

$$\Delta E_{\text{fused}} = E_{\text{fused}_{\text{fixed}}} + E_{\text{fused}_{\text{relaxed}}}$$

The predicted activation energy ($\Delta E^{\ddagger}_{\text{predict}}$) is finally defined by the sum of those relaxation energies $\Delta E_{\text{pyranose}}$ and ΔE_{fused} (usually negative) and the TS energy of the reference system ($\Delta E^{\ddagger}_{\text{ref}}$).

$$\Delta E^{\ddagger}_{\text{predict}} = \Delta E_{\text{pyranose}} + \Delta E_{\text{fused}} + \Delta E^{\ddagger}_{\text{ref}}$$

The inner strain energy ΔE_{strain} provides a simple relaxation indicator caused by endocleavage for a static conformation. The definition does not include the statistical distribution of several conformers of a pyranose ring. The effect of the inner strain caused by the two fused rings, independent of the effect of the conformational distribution by the fused ring restraining the pyranose ring, is an important point to discuss.

Using this model, the TS energies were predicted for pyranosides **2**−**9**. The TS energy relative to the β-anomer for **1** (139.0 kJ·mol^{-1}) was used as the reference activation energy $\Delta E^{\ddagger}_{\text{ref}}$.

The validation of the model was performed by comparing the predicted TS energies with those calculated via TS search along the C1−C2 torsion angle. The results were further assessed using the experimentally observed reactivity ranking.

3. RESULTS AND DISCUSSION

3.1. TS Analysis. Figure 5 shows the potential energies of the TS as well as of the α-anomer relative to the β-anomer for structures **1**−**4**, **6**, and **9** (Figure 3) obtained by TS search along the C1−C2

dx.doi.org/10.1021/ja201024a |J. Am. Chem. Soc. 2011, 133, 5610–5619

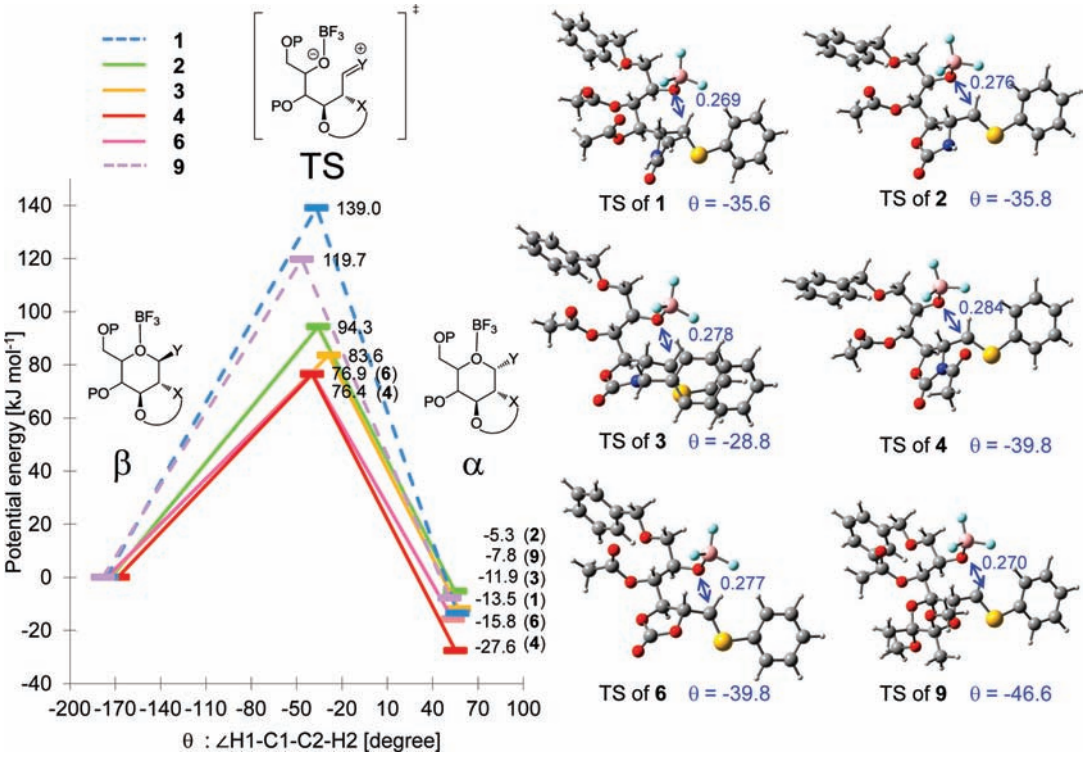

Figure 5. Results of the TS search for **1**−**4**, **6**, and **9** along the C1−C2 torsion angle as a reaction coordinate. For the pyranosides **2**−**4**, and **6**, which anomerize from the β- to the α-anomer, transition states appear at lower potential energies (solid lines). On the contrary, **1** and **9**, which experimentally do not undergo anomerization reactions, need to overcome higher TS energies (broken lines). The TS geometries are shown with the values of the C1−O5 bond length (in nm) and the H1−C1−C2−H2 torsion angle (in degrees).

bond rotation coordinate in the gas phase. The yields of the α- and β-anomers observed in experiments for **2**−**9** with $BF_3 \cdot OEt_2$ (2 equiv) in a CH_2Cl_2 solvent at −30 °C for 12 h are summarized in Table 1.

Transition states are located at around θ (H1−C1−C2−H2) = −30 ∼ −45 degrees (Figure 5). The TS of pyranosides with a five-membered fused ring at the 2,3-*trans* position (**2**−**4** and **6**; solid lines) are found to be lowest in energy (94.3, 83.6, 76.4, and 76.9 kJ·mol^{-1}). In the experiments, anomerization reaction was observed for all of these pyranosides (the α:β ratio in % is 19:69, 63:16, 75:0, and 14:46). On the contrary, the TS of pyranosides **1** and **9**, which do not undergo anomerization, are much higher in energy (139.0 and 119.7 kJ·mol; broken lines). Furthermore, the ordering of TS energies is in good agreement with the observed yields of the α-product. However, in comparison with the experiments, the TS of the pyranoside with carbonate **6** is estimated to be lower in energy. The C1−O5 bond lengths of the transition structures range from 0.269 to 0.284 nm. The energy calculations in a CH_2Cl_2 solvent estimated with an IEF-PCM scheme preserved the ordering of the potential energies, as mentioned in Section 2 (see Supporting Information for the details of the results). These results demonstrate that the TS analysis allows the qualitative estimation of the reactivity of anomerization.

For all compounds studied, the pyranoside rings keep a $^4C_1$ conformation along the reaction coordinate. According to the stereoelectronic effect theory, the *endo* C−O bond in the β-anomer adopting the $^4C_1$ conformation is advantageous for endocleavage.[12,13,16,19] This means that endocleavage of compounds **1b**-**9b** is favored by the $^4C_1$ conformation. However, they are split into the anomerizing and nonanomerizing groups showing a clear difference of the TS in energy. This indicates

Table 1. Experimental Yields of the α- and the β-Anomers, with $BF_3 \cdot OEt_2$ (2 equiv) in CH_2Cl_2 Solution at −30 °C for 12 h[a]

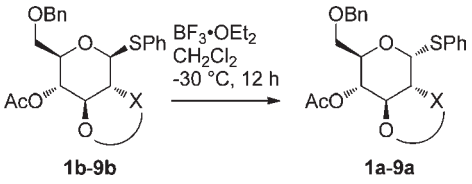

entry	reactant (β-anomer)	product yield (ratio) α-anomer **1a**−**9a** [%]	product yield (ratio) β-anomer **1b**−**9b** [%]
1	**1b**	0	93
2	**2b**	19	69
3	**3b**	63	16
4	**4b**	75	0
5	**5b**	80	0
6	**6b**	14	46
7	**7b**	0	92
8	**8b**	17	82
9	**9b**	0	61

[a] Entries 1−3 (**1**−**3**) and 6 (**6**) are reported in the literature.[29−31] Entries 4−5 (**4**−**5**) and 7−9 (**7**−**9**) were carried out for the present study (see Supporting Information for the experimental details).

dx.doi.org/10.1021/ja201024a |*J. Am. Chem. Soc.* 2011, 133, 5610–5619

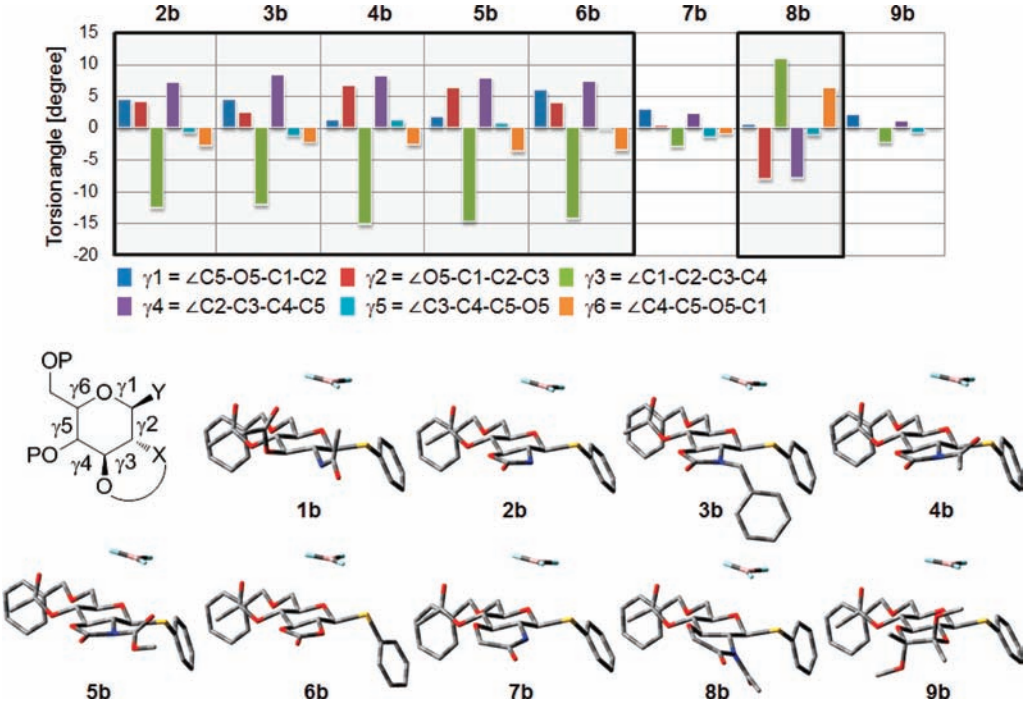

Figure 6. Deformation of pyranoside rings of **2b**−**9b** compared to **1b** ($^4C_1$).

the existence of an important factor other than the stereoelectronic effect enhanced by the $^4C_1$ conformation.

3.2. Deformation of the Pyranoside Rings in the Reactants (the *β*-Anomers). The torsion angles $\gamma 1-6$ of the pyranoside ring of **2b**−**9b** relative to **1b** are shown along with their structures in Figure 6. As can be seen from the geometries, the pyranoside rings all adopt a $^4C_1$ conformation. However, slight deformation was found in **2b**−**6b**, and **8b**, for which anomerization reactions were experimentally observed from the β- to the α-anomer. Pyranosides **7b** and **9b**, which do not anomerize, show almost no difference. For **2b**−**6b**, and **8b**, the largest deformation, by more than 10 degrees, appeared around the C2−C3 bond, $\gamma 3$ (C1−C2−C3−C4), where the cyclic protecting group is attached. In the course of the TS search along the C1−C2 bond rotation, those fused rings of **2b**−**6b**, and **8b** adopt a more planar conformation after endocleavage. Such a transition is not observed for the pyranosides **7b** and **9b**. These observations led us to assume that the strain from the fused ring preferring to be in a more planar conformation is a key factor for the enhancement of the reactivity of endocleavage.

3.3. Prediction of TS Energies from Inner Strain. Using the inner strain energy caused by the two fused rings (the pyranoside ring and the cyclic protecting group) defined in Figure 4, we derived TS energies $\Delta E^{\ddagger}_{predict}$. Figure 7 shows the comparison between the predicted TS energies $\Delta E^{\ddagger}_{predict}$ and the energies of the transition states located by the TS search $\Delta E^{\ddagger}$ (Figure 5) for **2**−**4**, **6**, and **9**. The prediction model based on inner strain successfully estimates TS energies ($\Delta E^{\ddagger}_{predict}$) very close to those from the TS search ($\Delta E^{\ddagger}$). The difference between the $\Delta E^{\ddagger}_{predict}$ and $\Delta E^{\ddagger}$ values ranges from 0.3 to 5.4 kJ·mol^{-1} (for **9** and **4**, respectively). The ordering of the TS energies stays the same: **4**−**6**−**3**−**2**−**9**.

The predicted TS energies $\Delta E^{\ddagger}_{predict}$ for **2**−**9** are validated using the experimental data in Table 1. Figure 8 graphically shows the comparison between the prediction and the experiments. The results are sorted in ascending order of the $\Delta E^{\ddagger}_{predict}$ values, that is, the ordering is from higher to lower reactivity:

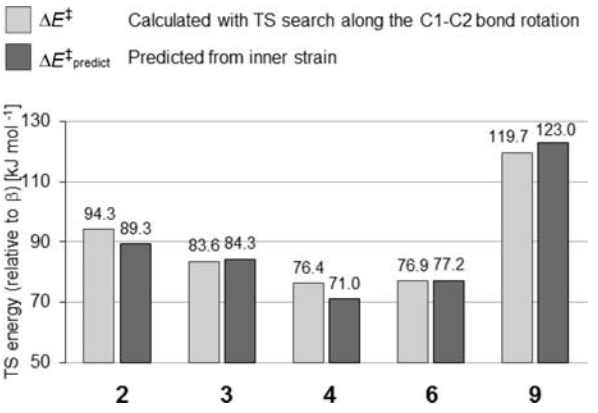

Figure 7. Validation of the predicted TS energies from inner strain $\Delta E^{\ddagger}_{predict}$. The $\Delta E^{\ddagger}_{predict}$ values are compared with the energies calculated by the TS search $\Delta E^{\ddagger}$.

4−**5**−**6**−**3**−**2**−**8**−**9**−**7**, shown in the left chart in Figure 8. The product ratios (β:α in %) in experiments with $BF_3 \cdot OEt_2$ (2 equiv.) in CH_2Cl_2 solution at −30 °C for 12 h (Table 1) are compared with the theoretically predicted reactivity, shown in the right chart in Figure 8, in which the white and black bars represent the ratios of the β- and α-anomers, respectively.

The difference in the predicted TS energy splits the model set of compounds into two groups. One is the group showing $\Delta E^{\ddagger}_{predict}$ values lower than 90 kJ·mol^{-1} (**2**, **3**, **4**, **5**, **6**, and **8**). The other group consists of **7** and **9**, showing $\Delta E^{\ddagger}_{predict}$ values higher than 120 kJ·mol^{-1}. We can see that, this grouping is in good agreement with the experiments: anomerization reaction occurs in the former group while it does not in the latter group. Good agreement is also found in the ordering between the $\Delta E^{\ddagger}_{predict}$ values and the experimental reactivity estimated based on the product ratios. Again, there is only one exception for the

dx.doi.org/10.1021/ja201024a |J. Am. Chem. Soc. 2011, 133, 5610–5619

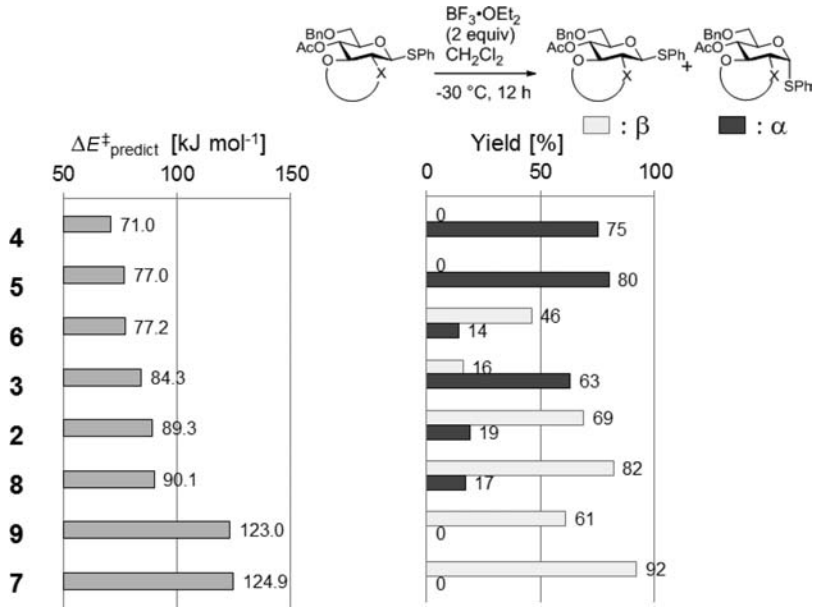

Figure 8. Validation of the predicted TS energies from inner strain. The ordering of TS energies predicted from the inner strain (left side) is compared with the experimental product ratios in Table 1 (right side).

Table 2. Experimental Yields of the α- and the *β*-Anomers for 4 and 5, with $BF_3 \cdot OEt_2$ (2 equiv) in CH_2Cl_2 Solution at −50 °C[a]

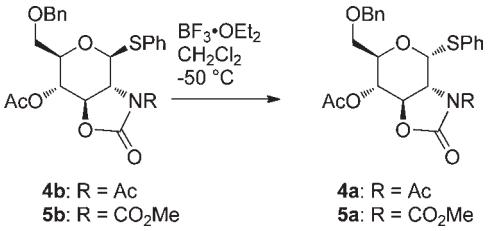

			product yield (ratio)	
entry	reaction time [hours]	reactant (*β*-anomer)	α-anomer **4a**−**5a** [%]	*β*-anomer **4b**−**5b** [%]
1	2	**4b**	67	19
2	4	**4b**	96	0
3	2	**5b**	0	97
4	4	**5b**	0	95

[a] See Supporting Information for the experimental details.

pyranoside with the carbonate protecting group **6**. The prediction overestimates the reactivity of **6** compared to the experiment.

For **4** and **5**, the lowest $\Delta E^{\ddagger}_{predict}$ values were obtained, suggesting high reactivity (71.1 (**4**) and 77.0 (**5**) kJ·mol^{-1}). In the experiments, these pyranosides anomerize perfectly, giving only the α-product in high yield at −30 °C for 12 h (75% and 80% for **4** and **5**, respectively, shown in Table 1). Under these reaction conditions, the yield of the α-product of **4** is 5% lower than **5** because of the lower solubility of the α-product of **4**, but the experiments at lower temperature −50 °C confirmed that **4** is more reactive than **5** (Table 2). Therefore, we conclude that the predicted theoretical reactivity for these pyranosides is in excellent agreement with the experiments.

Experiments demonstrate that the *N*-acetyl substituted cyclic protecting groups act as a strong promoter of the reaction (e.g., **4** and **8**). Out of the pyranosides **7b**−**9b**, with a six-membered cyclic protecting group attached, only **8b**, carrying the *N*-acetyl substituted cyclic protecting group, underwent anomerization to the α-anomer. The difference in the reactivity observed for **8** compared with **7** and **9** is also reflected by a large difference in the $\Delta E^{\ddagger}_{predict}$ values (89.9 (**8**), 124.9 (**7**) and 123.0 (**9**) kJ·mol^{-1}).

We want to further discuss the possibility of stereoelectronic effects related to the preferential conformation of pyranoside rings. The DFT calculations predict that the pyranoside ring is kept in a $^4C_1$ conformation along the reaction coordinate and the TS prediction was performed based only on the $^4C_1$ conformation for all pyranosides. The preference of a $^4C_1$ conformation is reasonable from a chemical point of view: in structures **2**−**8**, the pyranoside rings are restrained by the 2,3-*trans* cyclic protecting groups, while in structure **9** the $^4C_1$ conformation is stabilized by the double anomeric effects in the *trans*-decalin. The X-ray

dx.doi.org/10.1021/ja201024a |*J. Am. Chem. Soc.* 2011, 133, 5610–5619

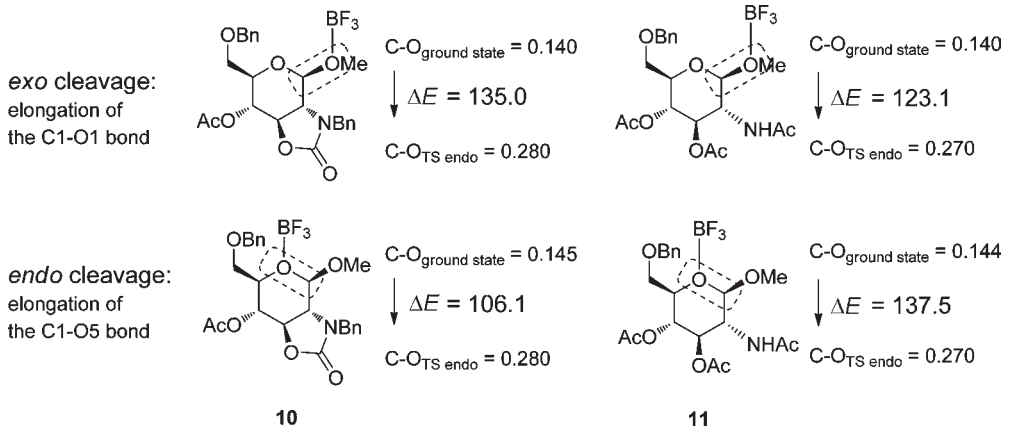

Figure 9. Energy profile associated with the *exo* vs *endo* cleavage. The amount of energy required to elongate the C−O bond from the ground state to the length at TS on the endocyclic pathway is calculated. The units of the length and the energy are presented in nm and kJ·mol^{-1}, respectively.

structures available for **3b** and **4b** are well reproduced by the calculations. If the stereoelectronic effect caused by the $^4C_1$ conformation was the predominant factor enhancing endocleavage, then a similarly high preference for endocleavage would be observed for all compounds. However, the TS prediction shows, in good agreement with the experiments, a clear *variation* in reactivity. The reactivity ordering is: protecting groups with an *N*-acetyl substituted 5-membered ring (**4**, **5**) > with a 5-membered ring (**2**, **3**, **6**) > with an *N*-acetyl substituted 6-membered ring (**8**) ≫ with a 6-membered ring (**7**, **9**) > without a cyclic protecting group (**1**). This ordering correlates with the *stiffness* of the $^4C_1$ pyranoside ring conformation, but calculations and experiments show that this is not enough to strongly enhance endocleavage. These results lead to the conclusion that the inner strain is the predominant factor enhancing the endocleavage-induced anomerization reactions. The stereoelectronic effect due to the restrained $^4C_1$ conformation is only a secondary factor.

3.4. Energy Profile of Exocyclic vs Endocyclic Cleavage. The experimental and theoretical investigations suggest that the anomerization reaction observed for this class of pyranosides occurs predominantly via the endocyclic pathway rather than the exocyclic pathway. In order to corroborate this assumption, we calculated the referential energy profile in the gas phase associated with the *exo* or *endo* cleavage for *O*-glycosides **10** and **11** (Figure 9).

The reference structures were generated via full geometry optimization, initiated from an ideal $^4C_1$ conformation. The *exo* C−O bond length is 0.140 nm for the optimized structures of **10** and **11**. The *endo* C−O bond lengths are 0.145 and 0.144 nm for **10** and **11**, respectively. The full geometry optimization preserved the $^4C_1$ conformation of the pyranoside rings. The energy profiles were then calculated by constrained geometry optimization, progressively elongating the *exo* or *endo* C−O bond (the C1−O1 or C1−O5 bond), in steps of 0.02 nm, from 0.15 to 0.28 nm for **10** and to 0.27 nm for **11**. The final bond lengths are close to the *endo* C−O bond lengths at TS (0.279 and 0.263 nm), found in the endocyclic pathway along the C1−C2 bond rotation.[28]

These energy profiles confirm the predominance of the *endo* cleavage of the pyranoside carrying a cyclic protecting group at the 2,3-*trans* position (Figure 9). For the pyranoside with the cyclic protecting group **10**, the amount of energy required to elongate the *endo* C−O bond from 0.145 to 0.280 nm is 106.1 kJ·mol^{-1}, while the amount of energy required to elongate the *exo* C−O bond from 0.140 to 0.280 nm is 135.0 kJ·mol^{-1}, ∼25 kJ·mol^{-1} larger than that for the *endo* C−O bond elongation. This means that *endo* cleavage is energetically favored in the pyranoside with the 2,3-*trans* cyclic protecting group. In contrast, higher energies are required for both of the elongations in the typical pyranoside **11**. For this pyranoside, the amount of energy required to elongate the *endo* C−O bond from 0.144 to 0.270 nm is 137.5 kJ·mol^{-1}, while the amount of energy required to elongate the *exo* C−O bond from 0.140 to 0.270 nm is 123.1 kJ·mol^{-1}, ∼15 kJ·mol^{-1} smaller than that for the *endo* C−O bond elongation. This means that *endo* cleavage is energetically less favorable in the pyranoside in the absence of a cyclic protecting group attached. These energy profiles also indicate that, for the pyranoside **11**, both cleavages would not be observed in mild conditions. As compared with **11**, in the cyclically protected **10**, the *endo* cleavage should be activated in mild conditions; however, it would be difficult for the *exo* cleavage to take place. The torsion angle $\gamma 3$ (C1−C2−C3−C4) of the optimized structures of **10** and **11** were −52.3 and −67.2 degrees, respectively. These results can be interpreted that *exo* cleavage is energetically favorable in the pyranoside with more planar $\gamma 3$ torsion angle. This trend is consistent with the findings by Crich and co-workers: the $^{O}H_5$ half-chair conformation, forming planar $\gamma 3$, reduces the energy barrier to cyclic oxacarbenium ion formation.[8,9,54]

Although mechanistic details of the exocyclic pathway as well as analyses in solution would allow the investigations of more precise behavior of the pyranosides, these simple pilot calculations support the relevancy of the predominance of the endocleavage in the anomerization reactions of pyranosides carrying 2,3-*trans* cyclic protecting groups. The inner strain caused by the fused rings is found to be the predominant factor to enhance the *endo* cleavage. However, this does not mean to rule out the possibility of the existence of other contributing factors. The fused rings can have an influence on the geometrical and electronic structures of pyranosides to diminish the effects enhancing *exo* cleavage,[55] for example, the ease of flattering of $\gamma 3$ (C1−C2−C3−C4), remote participation from a protecting group (e.g., at O3)[56], and stereoelectronic contributions.

Our computations suggest that, for pyranosides carrying 2,3-*trans* cyclic protecting groups, the barrier to *endo* cleavage ΔE_{endo} is approximately 20−40 kJ·mol^{-1} smaller than the barrier to *exo* cleavage ΔE_{exo}. In contrast, for normal pyranosides, ΔE_{endo} is

dx.doi.org/10.1021/ja201024a |*J. Am. Chem. Soc.* 2011, 133, 5610–5619

estimated to be larger than ΔE_{exo} with about a similar difference in energy. The theoretical model is in good agreement with experiments, which show, that under the selected mild reaction conditions using the week Lewis acid $BF_3 \cdot OEt_2$, the pyranosides carrying 2,3-*trans* cyclic protecting groups undergo an endocleavage-induced anomerization reaction. If stronger conditions are employed, e.g., a strong acid and/or higher temperature, these substrates can undergo anomerization also *via* the exocyclic pathway. Under these conditions, the normal pyranosides will undergo exocleavage-induced anomerization reaction. Employing a glycosylation promoter specifically attacking the sulfur at the anomeric site (S1) will also reduce the barrier to *exo* cleavage. This results in fast anomerization reactions via the exocyclic pathway, as reported by Boons and Stauch employing IDCP (iodonium dicollidine perchlorate) as a promoter.[57] Finally, our findings suggest that a careful selection of substrates, promoters, as well as reaction conditions will allow the control of the reactivity channel to either the exocyclic or endocyclic pathway. These findings will contribute to create new strategies for highly stereoselective synthesis to diversify oligosaccharides by controlling anomerization reactions.

4. CONCLUSIONS

Regarding anomerization reaction of the series of 4-*O*-acetyl-6-*O*-benzyl-thiophenylglycosides carrying 2,3-*trans* cyclic protecting groups, we formulated a simple model to predict TS energies from inner strain caused by the fused rings. Our model is an adaptation of Bickelhaupt's extended activation strain model for bimolecular reactions to unimolecular reaction systems. The predicted TS energy serves as a good reactivity predictor of the anomerization reaction from the β- to the α-anomer. The predicted reactivity is in a good agreement with the reactivity estimated from the TS search along the C1−C2 bond rotation coordinate, and also with the experiments. The energy profile calculations to estimate the feasibility of the elongation of the *endo*- or *exo* C−O bond indicate that endocleavage is energetically preferred in the pyranosides with 2,3-*trans* cyclic protecting groups. These series of investigations strongly support the endocyclic pathway as a reaction mechanism of the anomerization. The results lead to an important conclusion: the inner strain caused by the fused rings (the pyranoside ring and the cyclic protecting group) is the predominant factor for the enhancement of the endocleavage-induced anomerization. The stereoelectronic contribution to the endocleavage induced by the restrained conformation of pyranoside rings is a secondary factor. This inner strain model acts as a qualitative reactivity predictor, which can be calculated ~30 times faster than the TS search. This predictor is expected to be useful for further investigations, such as the virtual screening of compounds, possibly even at a molecular mechanics level. Furthermore, it will be an important concept in the discussion on the exocyclic vs endocyclic debate.

■ ASSOCIATED CONTENT

Supporting Information. Complete reference descriptions of ref 44, the number of imaginary frequencies for the transition states, geometries of the optimized α-and β-anomers and transition structures, transition state energies in a CH_2Cl_2 solvent using an IEF-PCM, the strain energies $\Delta E_{pyranose}$, ΔE_{fused}, and ΔE_{strain}, the experimental procedures, and the ^1H NMR and ^{13}C NMR spectral characteristics. This material is available free of charge via the Internet at http://pubs.acs.org.

■ AUTHOR INFORMATION

Corresponding Author
hsatoh@nii.ac.jp; smanabe@riken.jp

■ ACKNOWLEDGMENT

The present calculations were performed on Obelix, a computer cluster of the Competence Center for Computational Chemistry (C^4). H.S. and J.H. gratefully thank the Swiss National Science Foundation for funding this research with the International Short Visits Program. S.M. was supported by a Grant-in-Aid for Scientific Research (C) (Grant No. 21590036) from the Japan Society for Promotion of Science. S.M. thanks Ms. Akemi Takahashi for her technical assistance. We thank Professor David M. Birney (Texas Tech University, Lubbock, TX) and Professor Andrea Vasella (ETH Zurich, Switzerland) for valuable discussions.

■ REFERENCES

(1) Stallforth, P.; Lepenies, B.; Adibekian, A.; Seeberger, P. H. *J. Med. Chem.* **2009**, *52*, 5561–5577.
(2) Seeberger, P. H. *Nat. Chem. Biol.* **2009**, *5*, 368–372.
(3) Crich, D.; Chandrasekara, N. S. *Angew. Chem., Int. Ed.* **2004**, *43*, 5386–5389.
(4) Galonić, D. P.; Gin, D. Y. *Nature* **2007**, *446*, 1000–1007.
(5) Boltje, T. J.; Buskas, T.; Boons, G.-J. *Nature Chem.* **2009**, *1*, 611–622.
(6) Walvoort, M. T. C.; Dinkelaar, J.; van den Bos, L. J.; Lodder, G.; Overkleeft, H. S.; Codée, J. D. C.; Van der Marel, G. A. *Carbohydr. Res.* **2010**, *345*, 1252–1263.
(7) Mydock, L. K.; Demchenko, A. V. *Org. Biomol. Chem.* **2010**, *8*, 497–510.
(8) Crich, D. *Acc. Chem. Res.* **2010**, *43*, 1144–1153.
(9) Bohé, L.; Crich, D. *C. R. Chim.* **2011**, *14*, 3–16.
(10) Haworth, W. N.; Owen, L. N.; Smith, F. *J. Chem. Soc.* **1941**, 88–102.
(11) Gorenstein, D. G.; Findlay, J. B.; Luxon, B. A.; Kar, D. *J. Am. Chem. Soc.* **1977**, *99*, 3473–3479.
(12) Kirby, A. J. *Acc. Chem. Res.* **1984**, *17*, 305–311.
(13) Post, C. B.; Karplus, M. *J. Am. Chem. Soc.* **1986**, *108*, 1317–1319.
(14) Post, C. B.; Brooks, B. R.; Karplus, M.; Dobson, C. M.; Artymiuk, P. J.; Cheetham, J. C.; Phillips, D. C. *J. Mol. Biol.* **1986**, *190* (3), 455–479.
(15) Gupta, R. B.; Franck, R. W. *J. Am. Chem. Soc.* **1987**, *109*, 6554–6556.
(16) Guindon, Y.; Anderson, P. C. *Tetrahedron Lett.* **1987**, *28*, 2485–2488.
(17) McPhail, D. R.; Lee, J. R.; Fraser-Reid, B. *J. Am. Chem. Soc.* **1992**, *114*, 1905–1906.
(18) Liras, J. L.; Anslyn, E. V. *J. Am. Chem. Soc.* **1994**, *116*, 2645–2646.
(19) Deslongchamps, P.; Dory, Y. L.; Li, S. *Can. J. Chem.* **1994**, *72*, 2021–2027.
(20) Liras, J. L.; Lynch, V. M.; Anslyn, E. V. *J. Am. Chem. Soc.* **1997**, *119*, 8191–8200.
(21) Olsson, R.; Berg, U.; Frejd, T. *Tetrahedron* **1998**, *54*, 3935–3954.
(22) Deslongchamps, P.; Li, S.; Dory, Y. L. *Org. Lett.* **2004**, *6*, 505–508.
(23) Crich, D.; Vinod, A. U. *J. Org. Chem.* **2005**, *70*, 1291–1296.

(24) Boysen, M.; Gemma, E.; Lahmann, M.; Oscarson, S. *Chem. Commun.* **2005**, 3044–3046.
(25) Manabe, S.; Ishii, K.; Ito, Y. *J. Am. Chem. Soc.* **2006**, *128*, 10666–10667.
(26) O'Brien, C.; Poláková, M.; Pitt, N.; Tosin, M.; Murphy, P. V. *Chem.—Eur. J.* **2007**, *13*, 902–909.
(27) Olsson, J. D. M.; Eriksson, L.; Lahmann, M.; Oscarson, S. *J. Org. Chem.* **2008**, *73*, 7181–7188.
(28) Manabe, S.; Ishii, K.; Hashizume, D.; Ito, Y. *Acta Crystallogr.* **2008**, *E64*, o1868.
(29) Manabe, S.; Ishii, K.; Hashizume, D.; Koshino, H.; Ito, Y. *Chem.—Eur. J.* **2009**, *15*, 6894–6901.
(30) Satoh, H.; Hutter, J.; Lüthi, H. P.; Manabe, S.; Ishii, K.; Ito, Y. *Eur. J. Org. Chem.* **2009**, 1127–1131.
(31) Manabe, S.; Ito, Y. *Tetrahedron Lett.* **2009**, *50*, 4827–4829.
(32) Pilgrim, W.; Murphy, P. V. *J. Org. Chem.* **2010**, *75*, 6747–6755.
(33) Chipman, D. M.; Sharon, N. *Science* **1969**, *165*, 454–465.
(34) Ford, L. O.; Johnson, L. N.; Machin, P. A.; Phillips, D. C.; Tjian, R. *J. Mol. Biol.* **1974**, *88*, 349–360.
(35) Sinnott, M. L. *Chem. Rev.* **1990**, *90*, 1171–1202.
(36) Strynadka, N. C. J.; James, M. N. G. *J. Mol. Biol.* **1991**, *220*, 401–424.
(37) Hadfield, A. T.; Harvey, D. J.; Archer, D. B.; Mackenzie, D. A.; Jeenes, D. J.; Radford, S. E.; Lowe, G.; Dobson, C. M.; Johnson, L. N. *J. Mol. Biol.* **1994**, *243*, 856–872.
(38) McCarter, J. D.; Withers, S. G. *J. Am. Chem. Soc.* **1996**, *118*, 241–242.
(39) Bols, M. *Acc. Chem. Res.* **1998**, *31*, 1–8.
(40) The stereo-descriptors α and β are adopted to notate the stereochemistry at the anomeric site as defined by IUPAC conventions. The stereoselectivity is often described using relative stereo-descriptors to describe the configuration at the anomeric carbon, α and β, instead of the notation 1,2-*cis* and 1,2-*trans*. The α descriptor is used for the case where the OH at the anomeric carbon is on the same side as the OH at the reference atom in the Fischer projection, and the β descriptor is used for the opposite side. In the case of glucopranosides, the 1,2-*cis* and 1,2-*trans* positions are defined as the α and β configurations for the anomeric carbon, respectively. For more details, see the IUPAC definition at http://www.chem.qmul.ac.uk/iupac/2carb/06n07.html (accessed September 1, 2010).
(41) Kirby, A. J. *Stereoelectronic Effects*; Oxford University Press: New York, 1996.
(42) Becke, A. D. *J. Chem. Phys.* **1993**, *98*, 5648–5652.
(43) Stephenes, P. J.; Devlin, F. J.; Chabalowski, C. F.; Frisch, M. J. *J. Phys. Chem.* **1994**, *98*, 11623–11627.
(44) Frisch, M. J.; et al. *Gaussian 03, Revision C.02*; Gaussian, Inc.: Wallingford, CT, 2004.
(45) Peng, C.; Schlegel, H. B. *Israel J. Chem.* **1993**, *33*, 449–454.
(46) Peng, C.; Ayala, P. Y.; Schlegel, H. B.; Frisch, M. J. *J. Comput. Chem.* **1996**, *17*, 49–56.
(47) Tomasi, J.; Mennucci, B.; Cammi, R. *Chem. Rev.* **2005**, *105*, 2999–3093.
(48) Bickelhaupt, F. M. *J. Comput. Chem.* **1999**, *20*, 114–128.
(49) Diefenbach, A.; Bickelhaupt, F. M. *J. Chem. Phys.* **2001**, *115*, 4030–4040.
(50) Diefenbach, A.; de Jong, G. T.; Bickelhaupt, F. M. *Mol. Phys.* **2005**, *103*, 995–998.
(51) Diefenbach, A.; de Jong, G. T.; Bickelhaupt, F. M. *J. Chem. Theory Comput.* **2005**, *1*, 286–298.
(52) de Jong, G. T.; Bickelhaupt, F. M. *Chem. Phys. Chem.* **2007**, *8*, 1170–1181.
(53) van Zeist, W.-J.; Visser, R.; Bickelhaupt, F. M. *Chem.—Eur. J.* **2009**, *15*, 6112–6115.
(54) Crich, D.; Vinod, A. U.; Picione, J. *J. Org. Chem.* **2003**, *68*, 8453–8458.
(55) Demchenko, A. V. *Synlett* **2003**, 1225–1240.
(56) Baek, J. Y.; Lee, B.-Y.; Jo, M. G.; Kim, K. S. *J. Am. Chem. Soc.* **2009**, *131*, 17705–17713.
(57) Boons, G.-J.; Stauch, T. *Synlett* **1996**, 906–908.